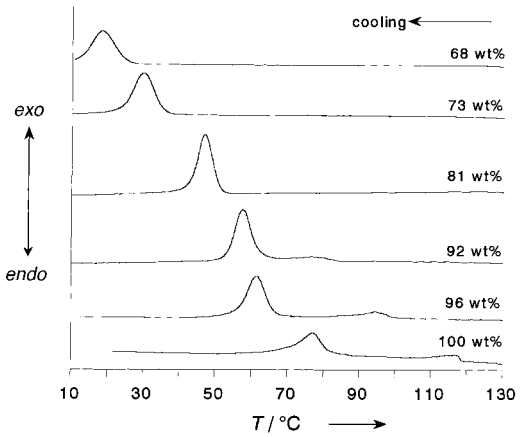

Figure 5. Differential scanning calorimetery thermograms for mixtures of DC-8 and 1,2-dichloroethane in different ratios (cooling rate 2 °C min^{-1}). The concentration of DC-8 is noted above each line.

afforded a cholesteric solid film. Although it is not clear how the solid film is constructed, it is likely that a nonequilibrated change in the concentration of the DC-8 solution on coating shifts the temperature region for the cholesteric phase to lower than that for the static thermotropic phase.

Experimental Section

Dicholesteryl esters DC-*n* ($n = 2-8, 10$) were synthesized by condensation of cholesterol and the corresponding diacids or by oxidizative coupling of the corresponding acetylene derivatives as reported.[7] MIKASA 1H-DX was used for spin-coating. The surface temperature of the substrate was controlled and monitored by a drier and an infrared thermometer (TASCO THI-400S), respectively. For bar coating, a wire bar (Tester Sangyo Co., Ltd.; no. 12) was used on a temperature-controlled stage (Iuchi THERMO PLATE TP-80).

Received: October 4, 1999 [Z14100]

[1] Recent reviews: a) M. Muthukumar, O. K. Ober, I. L. Thomas, *Science* **1997**, *277*, 1225–1232; b) G. Decher, *Science* **1997**, *277*, 1232–1237.
[2] a) E. T. Samulski, A. V. Tobolsky, *Nature* **1967**, *216*, 997; b) T. Tachibana, E. Oda, *Bull. Chem. Soc. Jpn.* **1973**, *46*, 2583–2584; c) J. Watanabe, S. Sasaki, I. Uematsu, *Polym. J.* **1977**, *9*(3), 337–340; d) G. Charlet, D. G. Gray, *Macromolecules* **1987**, *20*, 33–38; e) S. Shimamoto, D. G. Gray, *Chem. Mater.* **1998**, *10*, 1720–1726; f) W. Zhao, A. Kloczkowski, J. E. Mark, B. Erman, I. Bahar, *Macromolecules* **1996**, *29*, 2805–2812.
[3] S. Kwolek (du Pont), DE-B 1810426, **1970** [*Chem. Abstr.* **1970**, *72*, 112676t].
[4] Z. Wegner, *Z. Naturforsch. B* **1969**, *24*, 824–832.
[5] H. de Vries, *Acta Crystallogr.* **1951**, *4*, 219–226.
[6] I. Uematsu, Y. Uematsu in *Liquid Crystal Polymers I*, *Advances in Polymer Science 59* (Ed.: M. Gordon), Springer, Berlin, **1984**, pp. 37–73.
[7] N. Tamaoki, G. Kruk, H. Matsuda, *J. Mater. Chem.* **1999**, *9*, 2381–2384.

Al_{30}: A Giant Aluminum Polycation

Lionel Allouche, Corine Gérardin, Thierry Loiseau, Gérard Férey, and Francis Taulelle*

Aluminum hydrolysis plays a key role in strategic fields like catalysis, the Bayer process for aluminum production, geochemistry, soil science, water treatment, and material sciences. However, elucidation of all hydrolyzed aluminum species in solution has not yet been achieved.[1–8] Beyond the monomers $[Al(H_2O)_6]^{3+}$ and $[Al(OH)_4]^-$, only the Keggin polycation $[Al_{12}(AlO_4)(OH)_{24}(H_2O)_{12}]^{7+}$ (ε-Al_{13}) has been identified by X-ray diffraction (XRD)[9–10] and characterized in solution by ^{27}Al NMR. Several other species with hitherto unidentified ^{27}Al NMR signals at $\delta = 4$, 64.5, 70, and 76 were observed, along with broad signals in the 5–12 ppm range. Despite the numerous aforementioned studies, no new assignment has been established. In this in situ ^{27}Al NMR study, thermal treatment of a ε-Al_{13} solution evolves the new polycation $[Al_{30}O_8(OH)_{56}(H_2O)_{24}]^{18+}$ (Al_{30}). The $\delta = 70$ and 7–12 NMR signals are now definitely assigned to this species. The Al_{30} precipitated as a sulfate and its established structure consists of two δ-Al_{13} Keggin units linked by four AlO_6 octahedra. Although polyanions reach considerably larger sizes,[11] Al_{30} is unique by its size. It is the biggest polycation ever characterized, and the δ-Al_{13} units have never before been observed, neither in polycation nor polyanion chemistry.

Polycations are usually based on Keggin structures and described in polyoxometalate chemistry.[12–15] Keggin ions isomerize under five forms, α, β, γ, δ, and ε, shown in Figure 1a.

Tungstate and molybdate polyanions usually exhibit α- and β-Keggin structures (with or without cation vacancies) and can lead to pseudo-Keggin dimers by condensation.[12–15] Dimerisation has never been observed for aluminum polycations, but two polycationic Al_{13} Keggin isomers are known: α-Al_{13} in the mineral zunyite[16] and ε-Al_{13}.[9, 10, 17] The ε-Al_{13} polycation is obtained from hydrolysis of an aqueous $AlCl_3$ solution by NaOH at 95 °C with a hydrolysis ratio $m_h = [OH]/[Al]$ between 1.5 and 2.5. It has a central AlO_4 tetrahedron (narrow ^{27}Al NMR signal at $\delta = 63$), surrounded by twelve corner- and edge-sharing AlO_6 octahedra (very broad NMR signal around $\delta = 12$). The 1:12 Al^{IV}:Al^{VI} ratio between peaks at $\delta = 63$ and 12 confirms the polycation structure. The α-Al_{13} cation in zunyite[16, 18] (synthesized from aluminum hydroxide and silica under hydrothermal treatment at 300 °C) has

[*] Dr. F. Taulelle, L. Allouche, Dr. C. Gérardin
Laboratoire de RMN et Chimie du Solide
(UMR 7510 ULP-Bruker-CNRS)
Université Louis Pasteur
Institut Le Bel
4, rue Blaise Pascal
67070 Strasbourg Cedex (France)
Fax: (+33) 388-41-60-67
E-mail: taulelle@chimie.u-strasbg.fr
Dr. T. Loiseau, Prof. G. Férey
Institut Lavoisier
(IREM UMR 8637 CNRS)
Université de Versailles-Saint Quentin
45, Avenue des Etats-Unis
78035 Versailles Cedex (France)

  0570-0833/00/3903-0511 $ 17.50+.50/0

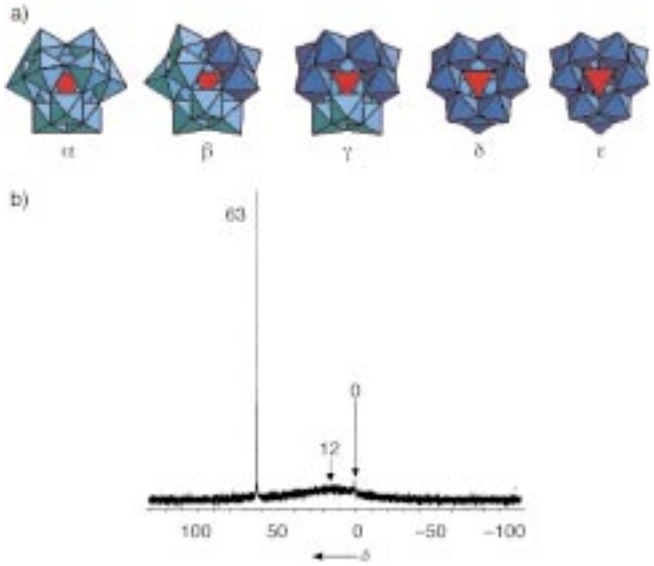

Figure 1. a) Keggin isomers after Baker and Figgis, showing AlO_4 tetrahedra (red) and AlO_6 octohedra (blue).[12] Isomeric differences (light blue/dark blue octohedra) arise from rotation of three adjacent AlO_6 octohedra through 60°. b) ^{27}Al NMR spectrum of aqueous ε-Al_{13}. The narrow peak at $\delta = 63$ corresponds to AlO_4 sites and the broad region around $\delta = 12$ corresponds to AlO_6 sites.

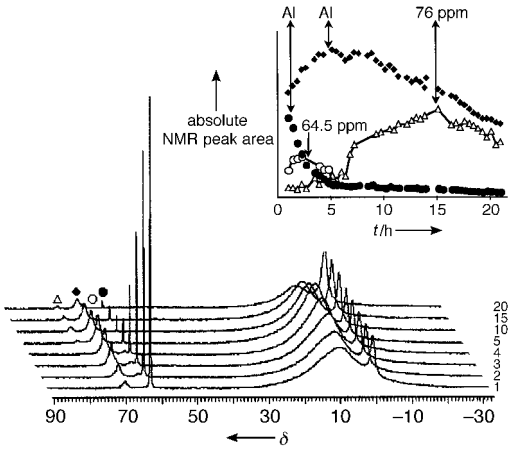

Figure 2. ^{27}Al NMR spectra of solution A over 20 h of thermal treatment at 127 °C. Inset: peak areas of the evolving signals of ε-Al_{13} at $\delta = 63$ (●), of $\delta = 64.5$ (○), of Al_{30} at $\delta = 70$ (◆), and of $\delta = 76$ (△). Scales for ○ and △ series have been multiplied sixfold for clarity.

its AlO_4 signal at $\delta = 72$[19] (observed by solid state MAS ^{27}-Al NMR) and a broad, unresolved ensemble of signals between 7 and 12 ppm, corresponding to the shell of AlO_6 octahedra.

Preliminary NMR experiments on the hydrolysis of $AlCl_3$ solutions at 95 °C agree with reported gel-permeation chromatography (GPC) results of Nazar et al.[8] and indicate that different species, not always assigned to known species, develop as a function of time. We therefore initiated in situ NMR studies of ε-Al_{13} solutions to observe signal evolution versus time at 95 or 127 °C. The results presented here only concern the 127 °C case, since an increase of temperature affects the rate of evolution but not the species formed.

In the first stage, conditions were established for obtaining clear solutions with exclusively the ε-Al_{13} polycation (solution A; see *Experimental Section*). The existence of ε-Al_{13} was confirmed by both liquid state ^{27}Al NMR (Figure 1b) and by powder X-ray diffraction after room temperature precipitation of the very insoluble ε-Al_{13} sulfate. A similar NMR examination of the species in solution and sulfate crystallization was the strategy used to characterize Al_{30}.

Evolution of ^{27}Al NMR signals from solution A at 127 °C (Figure 2) shows that thermal treatment causes ε-Al_{13} transformation into species containing aluminum in both tetrahedral and octahedral configurations. At $\delta = 70$ a signal increases at the expense of the $\delta = 63$ signal and becomes dominant after around 5 h at 127 °C (48 h at 95 °C). NMR signals at $\delta = 64.5$ and 76 appear during thermal treatment. The very weak $\delta = 64.5$ signal disappears when the $\delta = 70$ signal reaches its maximum. At this point, a $\delta = 76$ signal emerges. The signals of the octahedra at 5–12 ppm remain unresolved. Signals around $\delta = 0$ and in the 5–12 ppm region do not undergo any chemical exchange. At room temperature, monomeric $[Al(H_2O)_6]^{3+}$ appears at $\delta = 0$ (Figure 1b). At $\delta =$ 4 a signal is usually observed, this is still ambiguously assigned but most probably represents edge-sharing $[AlO_6]$ octahedra. Beyond 70 °C these two lines coalesce near $\delta = 0$ due to the large concentration of monomers. No chemical exchange takes place between signals in the 5–12 ppm and in the 0–4 ppm ranges. Signals for $[AlO_6]$ in the 5–12 ppm range are assigned to polycationic, external Keggin shells. This allows selective crystallization of the latter species.

After 5 h of heating at 127 °C (or 48 h at 95 °C), the solution (solution B) is brought back to room temperature; the ^{27}Al signals are considerably broader than in the 95 or 127 °C solutions. Some amounts of ε-Al_{13} are still present, but the spectrum is dominated by $\delta = 70$ and 10 components (Figure 3a).

To optimize crystallization, the influence of the sulfate-to-aluminum ratio y was investigated. According to its value, three new morphologies were obtained. Very small platelet- and ovoid-shaped crystals appear for high y values. Their structure determination is currently in progress. For $y = 0.3$, the large crystals corresponding to Al_{30} have a rhombohedral shape and were used for crystal structure determination (see *Experimental Section*).

After crystallization, an ^{27}Al NMR spectrum of the solution (Figure 3b) shows that most of the $\delta = 70$ and 10 signals have disappeared and the existence of almost only $[Al(H_2O)_6]^{3+}$ monomers ($\delta = 0$) in the remaining solution. Several rhombohedral crystals were collected and redissolved in water. The resulting solution exhibits a ^{27}Al NMR spectrum (Figure 3c) dominated by $\delta = 70$ and 10 signals, with two more signals at $\delta = 63$ and 0, from additional free ε-Al_{13} and from some monomers, respectively. Despite the presence of the latter signals, probably coming from intruding ε-Al_{13} crystals included during the selection of the rhombohedral ones or from some dissociation of Al_{30}, this result proves that $\delta = 70$ and 10 signals are indeed a signature of Al_{30}.

The crystal structure (see *Experimental Section*) reveals a new aluminum polycation with a formula $[Al_{30}O_8(OH)_{56}(H_2O)_{24}]^{18+}$ compensated by nine sulfate ions. The polycation (Figure 3d) results from the combination of two δ-Al_{13} units

  0570-0833/00/3903-0512 $ 17.50+.50/0

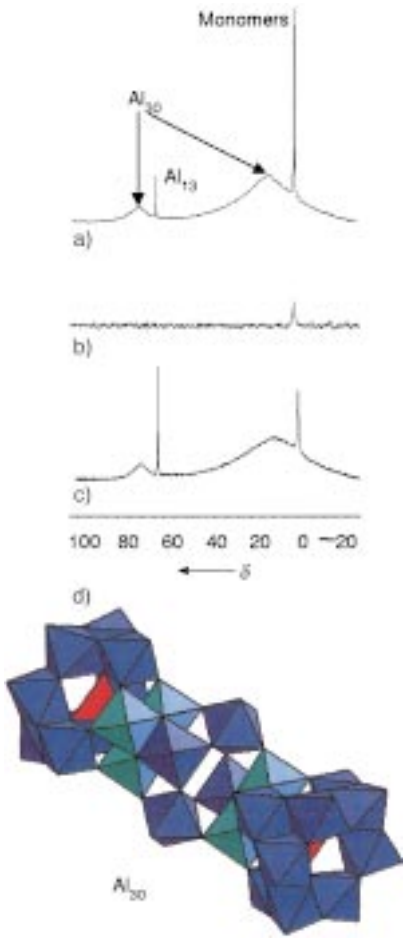

Figure 3. a) ^{27}Al NMR spectrum of solution B at room temperature. b) ^{27}Al NMR spectrum of solution B after precipitation of rhombohedral crystals. c) ^{27}Al NMR spectrum of the redissolved rhombohedral crystals in water. d) Polyhedral representation of $[\delta\text{-Al}_{13}]_2[\text{Al}_4(\text{OH})_8(\text{H}_2\text{O})_6]^{18+}$. Red = AlO_4, blue = AlO_6, the different shades represent the different Keggin configuration.

connected by a crown of four [AlO_6] octahedra. The formula of the solid is therefore rewritten $[(\delta\text{-Al}_{13})_2\{\text{Al}_4(\text{OH})_8(\text{H}_2\text{O})_6\}](\text{SO}_4)_9$.

From the structural study, Al_{30} formation may be described as follows. During the thermal treatment of ε-Al_{13}, some dissociate into AlO_6 monomers that subsequently add to undissociated ε-Al_{13}. These ε-Al_{13} species with one to three attached AlO_6 units (capped ε-Al_{13+1}, -Al_{13+2}, or -Al_{13+3}) are prone to isomerization into the respective δ forms. Once the isomerization is complete, the species may well be sufficiently stable to dimerize.

A correlation between the ^{27}Al NMR chemical shift of the tetrahedral aluminum and the average Al–O bond length in AlO_4 can be made. The chemical shifts of AlO_4 in ε-, δ-, and α-Al_{13} are $\delta = 63$, 70, and 72, respectively, whereas the corresponding mean Al–O distances decrease from 1.821 Å to 1.807 Å and 1.796 Å. This fits well to a linear relation: $d_{\text{Al–O}} = 1.98 - 0.0026 \times \delta$ (Å). The weak variation from $\delta = 63$ to 64.5, which may be commensurate with a variation in $d_{\text{Al–O}}$ of 0.004 Å, is too small to be attributed to an isomerization process. It is probably reasonable to assign that signal to the capped ε-Al_{13+1}, -Al_{13+2}, or -Al_{13+3} species. Isomerization of the latter species into the δ forms will lead to the $\delta = 70$ signal indistinguishable from that of the Al_{30}. Further thermal treatment may lead to a different isomer with a signal at $\delta = 76$. Zunyite, as we have already quoted, is synthesized at 300 °C. Its isomerization activation energy is probably higher. Thermal treatment at an increased temperature might lead to the formation of α-Al_{13} isomer, if concomitant stabilization by a proper anion occurs.

Nazar et al.[8] already observed the different tetrahedral species identified in this work. GPC allowed them to separate the aluminum species. It is worth noting that this elution sequence of the aluminium species is the same as the transformation sequence during the thermal treatment ($\delta =$ 63, 70, then 76; see Figure 2 inset). GPC ranks, therefore, the eluted species by their size for a given charge, providing a qualitative charge-to-mass (z/m) ratio selection. In this instance, charge-to-mass order parallels thermal stability. Species Al_{13}^{7+} and Al_{30}^{18+} exhibit a z/m ratio of 10.5×10^{-3} and 7.04×10^{-3} e g^{-1}, respectively. If the NMR signal at $\delta = 76$ would be assigned to α-Al_{13} isomer, known by GPC to have a smaller size than Al_{30} (but identical to that of ε-Al_{13}), it would imply for this species a charge of 4+ at most, and a z/m ratio smaller than 7.04×10^{-3} e g^{-1}. Conversely, the $\delta = 76$ signal might correspond to a larger polycation of proportionally greater charge. Further work on crystallization and structure determination of the $\delta = 76$ signal is needed to definitely solve the NMR assignments.

In situ ^{27}Al NMR and XRD have allowed us to see that a thermal treatment of an ε-Al_{13} solution produces a new aluminum cluster Al_{30}, which consists of two δ-Al_{13} Keggin units connected by a ring of four octahedral [AlO_6] units. The highly charged Al_{30} forms from hydrothermal treatment and appears as the second step of aluminum hydrolysis, after formation of ε-Al_{13}. It is the first time that a δ-Al_{13} unit, formed from the isomerization of ε-Al_{13}, is characterized. The heretofore unassigned ^{27}Al NMR signals at $\delta = 70$ and 10 were attributed to Al_{30}. Since Al_{30} is more temperature resistant and less sensitive to pH variations than ε-Al_{13}, this compound will certainly open new developments for elucidating the different species and the mechanisms involved in aluminum hydrolysis.[23]

Experimental Section

Synthesis: NaOH (2 M) was added dropwise to an $AlCl_3$ solution (0.3 M) maintained at 95 °C under fast stirring. The hydrolysis ratio was $m_h = 2.46$. The solution obtained (solution A) was cooled. The white precipitate, which formed when a drop of base was introduced into the $AlCl_3$ solution, redissolved immediately under stirring. At the end of the reaction, the solution was clear and contained only ε-Al_{13} (Figure 1b) and a few [AlO_6] monomers. Solution A was heated and stirred over 48 h at 95 °C or 5 h at 127 °C to form solution B. Solution B was stable for more than 6 months at room temperature. Crystallization was induced by addition of K_2SO_4 (0.5 M) to 5 mL of B up to a [SO_4]:[Al] ratio $y = 0.33$. After one week at room temperature, rhombohedral crystals appeared with millimeter dimensions.

NMR: ^{27}Al NMR has been run on a Bruker DSX-500 spectrometer at room temperature and on a Bruker AMX-400 spectrometer at 127 °C, with 130 and 104 MHz ^{27}Al resonating frequencies, respectively. A Bruker liquid probe BBO-10 mm, designed for a very low aluminum background signal, was used. At room temperature an NMR quartz tube is used. Above 100 °C,

  0570-0833/00/3903-0513 $ 17.50+.50/0

a "hydrothermal NMR tube"[20] is used instead. The reference $\delta = 0$ was to an external aqueous solution of $Al(NO_3)_3$ (1M).

X-ray crystal structure analysis: A crystal fragment was placed into a capillary Lindemann glass to prevent dehydratation. Intensities were recorded on a Bruker SMART CCD diffractometer ($Mo_{K\alpha}$ radiation $\lambda =$ 0.71073 Å, graphite monochromator) at 300 K. An empirical absorption correction was applied using the SADABS program.[21] 45869 unique reflections ($R_{int} = 0.0746$) were used ($1.31^\circ < \theta < 29.83^\circ$). The structure was solved and refined using the program package SHELXTL 5.03.[22] The examination of the systematic absences is consistent with the space groups *C*2/*c* (No. 15) or *Cc* (No. 9). The structure was first solved in the space group *C*2/*c*. Five sulfate groups were located from the observating successive Fourier map analyses. One SO_4^{2-} ion is placed nearby on the *2* axis (at 0, *y*, ¼), which induces a short S–S distance of 1.45 Å. A statistical disorder must occur for this SO_4^{2-} ion and the occupancy factor was refined to 50%; it corresponds to 4.5 SO_4^{2-} ions for 15 Al atoms (or nine SO_4^{2-} ions per Al_{30}). At this stage, some SO_4^{2-} groups were refined with geometrical restraints and water molecules were located approximately due to their very diffuse average electronic density. The sulfate counterions may not all be accurately positioned. With such a strategy the structure can be described as follows: $Al_{30}O_8(OH)_{56}(H_2O)_{24}(SO_4)_9 \cdot x\,H_2O$ ($x > 35$), monoclinic, space group *Cc* (No. 9), $a = 28.0259(5)$, $b = 19.4890(3)$, $c =$ 28.9883(5) Å, $\beta = 112.514(1)^\circ$, $V = 14626.6(4)$ Å^3, $Z = 4$, $\rho_{calc} =$ 1.588 g cm^{-3}, $\mu = 0.452$ mm^{-1}, crystal size $0.38 \times 0.26 \times 0.12$ mm^3. Crystallographic data (excluding structure factors) for the structure reported in this paper have been deposited with the Fachinformationszentrum Karlsruhe. Further details may be obtained from FIZ, 76344 Eggenstein-Leopoldshafen, Germany (fax: (+49) 7247-808-666; e-mail: crysdata @fiz-karlsruhe.de) on quoting the depository number CSD-410995.

Received: October 7, 1999 [Z14125]

[1] a) J. W. Akitt, J. M. Elders, X. L. R. Fontaine, A. K. Kundu, *J. Chem. Soc. Dalton Trans.* **1989**, 1889–1895; b) J. W. Akitt, J. M. Elders, X. L. R. Fontaine, A. K. Kundu, *J. Chem. Soc. Dalton Trans.* **1989**, 1897–1901.

[2] J. P. Jolivet in *De la Solution à l'Oxyde (*Eds.: M. Henry, J. Livage*)*, CNRS, Paris, **1994**.

[3] J. Y. Bottero, D. Tchoubar, J. M. Cases, F. Flessinger, *J. Phys. Chem.* **1982**, *86*, 3667–3673.

[4] a) D. R. Parker, P. M. Bertsch, *Environ. Sci. Technol.* **1992**, *26*, 908–914; b) D. R. Parker, P. M. Bertsch, *Environ. Sci. Technol.* **1992**, *26*, 914–921.

[5] P. H. Hsu, *Clays Clay Miner.* **1997**, *45*, 286–289.

[6] R. C. Turner, *Can. J. Chem.* **1976**, *54*, 1910–1915.

[7] a) J. T. Kloprogge, D. Seykens, J. W. Geus, J. B. H. Jansen, *J. Non-Cryst. Solids* **1992**, *142*, 87–93; b) J. T. Kloprogge, D. Seykens, J. W. Geus, J. B. H. Jansen, *J. Non-Cryst. Solids* **1992**, *142*, 94–102.

[8] L. F. Nazar, G. Fu, A. D. Bain, *Chem. Mater.* **1991**, *3*, 602–610.

[9] G. Johansson, *Acta Chem. Scand.* **1960**, *14*, 771–773.

[10] G. Johansson, G. Lundgren, L. G. Sillen, R. Söderquist, *Acta Chem. Scand.* **1960**, *14*, 769–771.

[11] A. Müller, S. Q. N. Shah, H. Bogge, M. Schmidtmann, *Nature* **1999**, *397*, 48–50.

[12] L. C. W. Baker, J. S. Figgis, *J. Am. Chem. Soc.* **1970**, *92*, 3794–3797.

[13] M. T. Pope, A. Müller in *Polyoxometalates: From Platonic Solids to Anti-Retroviral Activity,* Kluwer Academic, Dordrecht, **1994**.

[14] C. L. Hill, *Chem. Rev.* **1998**, *98*, 1–390.

[15] K. Wassermann, R. Knut, H. J. Lunk, J. Fuchs, N. Steinfeld, R. Stösser, *Inorg. Chem.* **1995**, *34*, 5029–5036.

[16] L. Z. Pauling, *Kristallokhim. Miner.* **1933**, *84*, 442.

[17] W. O'Neil Parker, R. Millini, I. Kiricsi, *Inorg. Chem.* **1997**, *36*, 571–575.

[18] G. Turco, PhD thesis, Université de Nice (France), **1962**.

[19] A. C. Kunwar, A. R. Thompson, H. S. Gutowsky, E. Oldfield, *J. Magn. Reson.* **1984**, *60*, 467–472.

[20] C. Gerardin, M. In, F. Taulelle, *J. Chim. Phys. Phys. Chim. Biol.* **1995**, *92*, 1877.

[21] G. M. Sheldrick, SADABS (the Siemens Area Detector ABSorption correction), University of Göttingen, **1996**.

[22] G. M. Sheldrick, SHELXTL 5.03, Bruker Analytical X-ray Systems, Madison, WI, **1994**.

[23] During submission of this contribution L. F. Nazar, Waterloo University, Canada mentioned her findings of an isolated Al_{13} δ-Keggin isomer and of an Al_{30} cluster.

The Vibrational Inelastic Neutron Scattering Spectrum of Dodecahedrane: Experiment and DFT Simulation**

Bruce S. Hudson,* Dale A. Braden, Stewart F. Parker, and Horst Prinzbach

Because of its high symmetry (I_h) the hydrocarbon dodecahedrane ($C_{20}H_{20}$)[1–4] provides a classic case for vibrational analysis and, as a result, a rigorous test of the methods of ab initio or density functional normal-mode analysis. Under the I_h point group the 114 normal modes of vibration are classified into $2A_g + 1T_{1g} + 2T_{2g} + 4G_g + 6H_g + 3T_{1u} + 4T_{2u} + 4G_u + 4H_u$ symmetry types. There are only 30 discrete vibrational frequencies due to the high average degeneracy. Of these only the $3T_{1u}$ modes are active in the IR spectrum and only the $2A_g$ and $6H_g$ modes are active in the Raman spectrum. Thus 19 of the 30 modes of vibration are unobservable by these optical methods so long as this molecule retains its high symmetry.

Inelastic neutron scattering (INS) spectroscopy is not subject to the restrictions of optical selection rules. This permits all modes to be observed in proportion to the extent to which hydrogen-atom motions contribute to that mode. From a set of calculated normal-mode eigenvectors and

[*] Prof. B. S. Hudson
Department of Chemistry, Syracuse University
Syracuse, NY 13244-4100 (USA)
Fax: (+1) 315-443-4070
E-mail: bshudson@syr.edu

D. A. Braden
Department of Chemistry, University of Oregon
Eugene, OR 97403 (USA)

Dr. S. F. Parker
ISIS Facility, Rutherford Appleton Laboratory
Chilton, Didcot OX 11 0QX (UK)

Prof. H. Prinzbach
Chemisches Laboratorium der Universität
Institut fur Organische Chemie und Biochemie
79104 Freiburg (Germany)

[**] The Rutherford Appleton Laboratory is thanked for access to neutron beam facilities at ISIS. This work was partially supported by the US National Science Foundation (grant CHE 9803058) and utilized the computer systems Exemplar and SGI PCarray at the National Center for Supercomputing Applications, University of Illinois at Urbana-Champaign. We thank Chris Middleton of Syracuse University for development of the program used to plot neutron spectra.

  0570-0833/00/3903-0514 $ 17.50+.50/0